The Astrophysical Journal, 850:111 (7pp), 2017 December 1 https://doi.org/10.3847/1538-4357/aa9481

Optical, Near-IR, and X-Ray Observations of SN 2015J and Its Host Galaxy*

A. A. Nucita[1,2], F. De Paolis[1,2], R. Saxton[3], V. Testa[4], F. Strafella[1,2], A. Read[5], D. Licchelli[1], G. Ingrosso[1,2], F. Convenga[1], and K. Boutsia[6]
[1] Department of Mathematics and Physics "E. De Giorgi", University of Salento, Via per Arnesano, CP 193, I-73100, Lecce, Italy; nucita@le.infn.it
[2] INFN, Sez. di Lecce, Via per Arnesano, CP 193, I-73100, Lecce, Italy
[3] European Space Astronomy Centre, SRE-O, P.O. Box 78, E-28691, Villanueva de la Cañada (Madrid), Spain
[4] INAF, Osservatorio Astronomico di Roma, via Frascati 33, I-00078 Monte Porzio Catone, Italy
[5] Department of Physics and Astronomy, Leicester University, Leicester LE1 7RH, UK
[6] Carnegie Observatories, Las Campanas Observatory, Colina El Pino, Casilla 601, La Serena, Chile
Received 2017 May 30; revised 2017 October 3; accepted 2017 October 14; published 2017 November 22

Abstract

SN 2015J was discovered on 2015 April 27th and is classified as an SN IIn. At first, it appeared to be an orphan SN candidate, i.e., without any clear identification of its host galaxy. Here, we present an analysis of the observations carried out by the VLT 8 m class telescope with the FORS2 camera in the *R* band and the *Magellan* telescope (6.5 m) equipped with the IMACS Short-Camera (*V* and *I* filters) and the FourStar camera (*Ks* filter). We show that SN 2015J resides in what appears to be a very compact galaxy, establishing a relation between the SN event and its natural host. We also present and discuss archival and new X-ray data centered on SN 2015J. At the time of the supernova explosion, *Swift*/XRT observations were made and a weak X-ray source was detected at the location of SN 2015J. Almost one year later, the same source was unambiguously identified during serendipitous observations by *Swift*/XRT and *XMM-Newton*, clearly showing an enhancement of the 0.3–10 keV band flux by a factor ≃30 with respect to the initial state. *Swift*/XRT observations show that the source is still active in the X-rays at a level of ≃0.05 counts s^{-1}. The unabsorbed X-ray luminosity derived from the *XMM-Newton* slew and *SWIFT* observations, $L_x \simeq 5 \times 10^{41}$ erg s^{-1}, places SN 2015J among the brightest young supernovae in X-rays.

Key words: supernovae: individual (SN 2015J)

Supporting material: data behind figure

1. Introduction

It is not obvious that supernova (SN) events may occur in a location of the sky without any associated host galaxy. As a matter of fact, the Sternberg Astronomical Institute supernova catalog (Tsvetkov et al. 2004), reports more than 5000 such events whose nature needs to be addressed. In this respect, there is certainly the possibility that the host galaxy is not detected in the majority of the cases because of its low surface brightness, or there is a more challenging hypothesis: the SN progenitors are hyper-velocity stars characterized by velocities as large as ≃700–1000 km s^{-1} (see e.g., Brown et al. 2005, 2014; Martin 2006; Brown 2011) that have escaped their host galaxies. In both cases, these supernovae are labeled as *orphan SN events*, unless the host galaxy is identified in follow-up observations.

SN 2015J is a supernova[7] that occurred on 2015 April 27th at the (J2000) coordinates R.A. = 07^h:35^m:$05^s.18$ and decl. = −69°:07′:53″.1 and observed for the first time by Childress et al. (2015) with the 268 megapixel camera on the SkyMapper 1.3 m telescope at Siding Spring Observatory (Australia) as part of the SkyMapper Transient (SMT) survey (Scalzo et al. 2017). Source images acquired on 2015 April (27.9 UT) had both *g* and *r* magnitudes of 19.3.

The SN light curve showed an initial peak of $r = 18.2$ on May (08.9 UT) before declining. The light curve then rose again up to a second peak at $r = 16.8$ on June 09.9 UT. After a brief decline, it rose again, and as noted by the same authors (to whom we refer for more details), the last observation showed a magnitude of $r \simeq 16.0$ still rising. Childress et al. (2015) also acquired a 20-minute spectrum with the Wide Field Spectrograph (WiFeS, Dopita et al. 2007), which revealed an SN IIn[8] located at redshift $z = 0.0054$, corresponding to a distance of ≃24.2 Mpc (adopting the more recent cosmological parameters $H_0 = 67.15$ km s^{-1} Mpc^{-1}, $\Omega_M = 0.27$, and $\Omega_\Lambda = 0.73$).

The target was also observed with the Australia Telescope Compact Array on 2015 June (29.1 UT) (Ryder et al. 2015), revealing a radio source at a position consistent with that measured optically, and with fluxes of 0.07 ± 0.02 mJy and 0.10 ± 0.03 mJy at frequencies of 9.0 and 5.5 GHz, respectively.

When searching for an optical counterpart, Childress et al. (2015) found no obvious host galaxy close to the supernovae location and noted that SN 2015J might be associated with a group of galaxies at similar redshifts. In particular, NGC 2434 (at $z = 0.004637$ as given by NED) is at a projected distance of 62 kpc and NGC 2442 ($z = 0.004890$ via NED) is at 166 kpc. In addition, SN 2015J is close to a 10^9 $M_\odot$ gas cloud (HIPASS J0731-69, see Ryder et al. 2001). NGC 2442 seems to interact

* Based on observations obtained with *XMM-Newton*, an ESA science mission with instruments and contributions directly funded by ESA Member States and NASA, with ESO Telescopes at the La Silla-Paranal Observatory under program ID 298.D-5016(A), and with the 6.5 m Magellan Telescopes located at Las Campanas Observatory, Chile. We also acknowledge the use of public data from the *Swift* data archive.
[7] The source is also labeled as SMTJ07350518-6907531.
[8] SNe IIn are characterized by narrow emission Balmer lines in their spectra (Filippenko 1997) and show signatures of the interaction between the SN ejecta and the circumstellar medium (see, e.g., Schlegel 1990). They form a heterogeneous object sample, as their peak luminosities (which span more than two orders of magnitude; Richardson et al. 2014) depend on many factors, such as the circumstellar medium density, the SN ejecta mass, and input energy.

with HIPASS J0731-69 and the whole complex can be considered as the result of a previous gravitational interaction. However, the two galaxies are too far to explain SN 2015J as originating from a hyper-velocity star progenitor that escaped one of them. It is then natural to expect that the SN occurred in a faint and small galaxy not previously identified.

To address this issue, we obtained $\simeq$0.98 hr of net exposure time on the VLT 8 m class telescope with the FORS2 camera in the *R* filter and a few exposures (180 s each) from the *Magellan* telescope (6.5 m) with the IMACS Short-Camera in the *V* and *I* filters, and with the FourStar camera in the *Ks* band. The analysis of these observations, presented in this paper, allowed us to definitively show that SN 2015J resides in what appears to be a very compact galaxy, finally establishing a relation between the SN event and its natural host. After comparing the newly acquired data with archival data (as the Digital Sky Survey—DSS—blue and infrared images[9] and the Catalina Sky Survey—CSS—data[10]) we realized that, prior to the SN explosion, the light of the SN progenitor contributed in a non-negligible way to the host galaxy brightness (see Section 2 for details).

SN IIn events are among the most luminous X-ray supernovae (see, e.g., Chandra et al. 2012a, 2015), and indeed X-ray observations give important information about the SN itself and its environment. Since 2004, the region of the sky around SN 2015J had been observed many times by the *XMM-Newton* satellite in slew mode, but without yielding any detections. The *Chandra* observatory also did not detect any X-ray source during past observations. At the time of the supernova explosion, *Swift*/XRT observations were made and a weak source of X-rays was detected at the location of SN 2015J. Almost one year later, the same source was clearly identified during serendipitous observations by *Swift*/XRT and *XMM-Newton*, showing an enhancement of the 0.3–10 keV band flux by a factor $\simeq$30 with respect to the initial state. We requested new *Swift*/XRT observations, which, performed on 2017 March and July, clearly showed that the source is still active in the X-rays at a level of $\simeq$0.05 counts s^{-1}, as will be discussed in Section 3.

The paper is organized as follows. In Section 2, we report on archival (DSS and CSS) and newly acquired (VLT/FORS2 and *Magellan*/IMACS/FourStar) data, leaving to Section 3 the analysis of all the available X-ray data. We present our conclusions in Section 4.

2. SN 2015J: Optical and near-IR Data

The absence of a clear identification of the SN 2015J host galaxy makes the event a possible orphan SN candidate. With the aim of determining if any extended optical counterpart does exist, we searched for past DSS images acquired in the direction of the target. At the coordinates of the supernova explosion, a source was clearly identified in the DSS survey in the J_{ph} (340–590 nm), F_{ph} (590–715 nm), and N_{ph} (700–970 nm) images. In Figure 1 (left panel), we show the image in the F_{ph} band of the DSS field toward the SN 2015J. The red circle (with radius of $\simeq 1''$) is centered on the nominal coordinates of SN 2015J.

The *Catalogs and Surveys Branch* of the Space Telescope Science Institute digitized the photographic plates from the DSS to produce the Guide Star Catalog, which ultimately contains positions, proper motions, classifications, and magnitudes in multiple bands for almost a billion objects down to approximately $J_{ph} = 21$ and $F_{ph} = 20$. The source identified at the SN position has magnitudes in the photographic bands F_{ph}, J_{ph}, and N_{ph} of 18.29, 19.61, and 18.26, respectively.

The source identified in the DSS images appears to be point-like and very faint, thus presenting two possibilities: the DSS source is the unresolved SN 2015J host galaxy, or, in the orphan supernovae scenario (Zinn et al. 2012), it is the progenitor of SN 2015J, which is believed to be an Eta-Carinae like star (see, e.g., Gal-Yam et al. 2007), which, having an absolute magnitude of $\simeq -12$ at the distance of $\simeq$24.2 Mpc (same as that of the observed supernova), would have a visual magnitude of about 19.5, not far from that corresponding to the DSS source.

To distinguish between these two possibilities, we requested observing time at the VLT telescope equipped with the FORS2 camera in the *R* filter (550–800 nm) and at the *Magellan* telescope with the IMACS (*V* and *I* filters) and FourStar (*Ks* filter). As far as the VLT/FORS2 data is concerned, each single frame (acquired in 2016 December) was corrected using standard procedures (bias, dark current, and flat-field corrections) and then geometrically aligned in order to get a calibrated and clean image (in counts s^{-1}) as an averaged sum. The VLT/FORS2 *R* band image resulted in a total exposure time of 0.98 hrs. In Figure 1 (right panel), we provide a zoom-in (with histogram equalization) around the target. The green circles (each with a $0\farcs5$ radius and centered on the centroid of the corresponding brightness surface) in the right panel correspond to some of the sources detected in the the VLT/FORS2 image using the SExtractor code. We extracted the aperture photometry with a source extraction radius of $\simeq 4''$ (i.e., well above the FWHM of the FORS2 camera), while the background was evaluated locally. After calibrating the photometry with the GSC2.3 catalog (although the photographic band of the DSS plates is similar (but not exactly the same) to the FORS2 *R* band), the target source resulted in a magnitude (Vega system) in the *R* band of 18.80 ± 0.20. The target appeared in the VLT image as a clearly extended source, and we verified its extension by deriving the point-spread function (PSF) of the frame using the DAOPHOT package (Stetson 1987). In particular, we invoked the *find* and *photometry* routines in order to determine the position and aperture photometry of any source above a certain background threshold. We then selected an adequate number of round and isolated (likely PSF) stars. Hence, the DAOPHOT *psf* routine allowed us to estimate an image PSF characterized by a FWHM of $\simeq 0\farcs65$. After subtracting the PSF from the image, we were left with an image of residuals (Figure 2) in which all the star-like objects are removed. Note that large deviations (from what are expected for a point-like object) appear at the location of the source and this is convincing evidence that we are dealing with an extended object.[11]

[9] The Digitized Sky Survey comprises a set of all-sky photographic surveys with the Palomar and UK Schmidt telescopes. The DSS data may be retrieved from http://archive.eso.org/dss/dss.

[10] The CSS, which uses a 1.5 m telescope on the peak of Mt. Lemmon and a 68 cm telescope near Mt. Bigelow (both in the Tucson area, USA), is a project to discover comets and asteroids and to search for near-Earth objects (NEOs). Further information on the CSS project is available at https://catalina.lpl.arizona.edu/.

[11] Note that a diffuse brightness surrounds the target, and based on the K image of Figure 3, an emission peak (the *knot* with a magnitude of 18.77 ± 0.18) is also present in a position located southeast from the core.

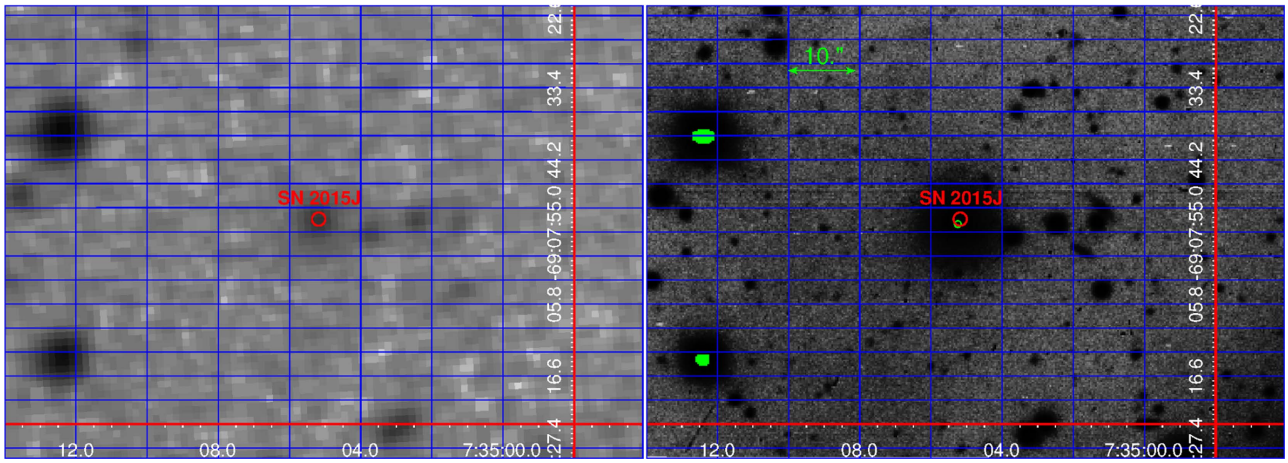

Figure 1. The DSS $F_{\rm ph}$ band image (left panel) and the image acquired by the VLT/FORS2 in the *R* band (right panel) of the region toward SN 2015J are shown. The red circle is centered on SN 2015J. The green circle (with a 0.″5 radius and centered on the centroid of the corresponding brightness surface) appearing in the right panel corresponds to the source detected inthe VLT/FORS2 image.

The SExtractor code classified the target as a galaxy (with an ellipticity parameter 0.127 and S/G classifier output of 0.03). The extraction radius used in order to encompass the visible halo of the galaxy is $\simeq 4''$, corresponding to a linear length of $\simeq$0.5 kpc for an estimated distance of 24.2 Mpc as that of SN 2015J.

The distance between SN 2015J and the centroid coordinates of the closest source detected in the FORS2 image is $\simeq 0.''8$.

The IMACS and FourStar images were reduced following standard procedures, which allowed us to estimate the *V*, *I*, and *Ks* magnitudes (Vega system) of the host galaxy (possibly with a contribution of the SN; see next discussion) to be 19.68 ± 0.07, 18.61 ± 0.08, and 15.80 ± 0.15, respectively. Note that the photometry of the *K* band image was obtained by calibrating the 2MASS catalog sources found within the field of view, while the *V* and *I* magnitudes were calibrated using the standard stars in Landolt field RU149 observed on the same night. As an example, Figure 3 shows a zoom-in of the field of view around the target as appearing in the FourStar *Ks* band.

From the discussion above, the presence of the SN host galaxy is evident, thus supporting the scenario of SN 2015J being a normal SN that occurred in a compact galaxy at a distance of about 24.2 Mpc. As a last remark on the host galaxy, note that inNASA's *Wide-field Infrared Survey Explorer* (Wright et al. 2010) all-sky data, a source was detected in 2010, i.e., well before the supernova explosion. The source had *W1* (3.4 μm) and *W2* (4.6 μm) magnitudes of $\simeq$15.91 and $\simeq$15.89, respectively.

The multi-band light curve of the target including the CSS data, the data acquired during the SN event (as extracted from the figures in Childress et al. 2015), and the data obtained from VLT and MAGELLAN, is shown in Figure 4. The inset shows a zoom-in of the light curve about the time of the SN event, with the black arrow indicating the time of the SN explosion. The comparison between the *V*-band magnitude as estimated from the *Magellan* IMACS data ($\simeq 19.68 \pm 0.07$) and the mean value observed in the CSS data before the SN explosion ($\simeq 18.52 \pm 0.45$) allow us to conclude that the progenitor of the SN event contributed in a non-negligible way to the host galaxy brightness. In particular, we find $F_{\rm PSN}/F_{\rm G} \simeq 1.9$,$F_{\rm PSN}$ and $F_{\rm G}$ being the fluxes of the pre-SN event and host galaxy, respectively.

3. SN 2015J: the X-Ray view

The location of SN 2015J was observed in several *XMM-Newton* slews since 2004 but no source was detected. A *Chandra* observation (OBs ID 2923 antecedent to the SN) did not detect any X-ray source at the position of SN 2015J and put an upper limit on the quiescent X-ray flux of $F_{0.2-8{\rm keV}} \simeq 6 \times 10^{-15}\,{\rm erg\,cm^{-2}\,s^{-1}}$, about 100 times deeper than the *XMM-Newton* slew upper limits.

SN 2015J was observed by *Swift*/XRT on several occasions soon after the SN explosion (see Table 1). The *Swift* data have been analyzed using the standard procedures described in Burrows et al. (2005) with the latest calibration files. We processed the XRT data with the *XRT-Pipeline* (v.0.12.6) task and we applied standard screening criteria using the FTOOL (Heasoft v. 6.19). The source spectra have been extracted from a circular region centered on the target nominal coordinates (with a radius of 40 arcsec) using the *xselect* routine, while the background spectra were obtained from an annulus with external an radius of 60 arcsec. We then used the *xrtmkarf* script to create the ancillary response files and imported the grouped spectra within *XSPEC* (Arnaud et al. 2007) for the spectral analysis.

As shown in Table 1, the *Swift*/XRT count rate of the target source was $\simeq 7.0 \times 10^{-3}$ counts s^{-1} in the 0.3–10 keV energy band during the SN explosion (2015 August 26th, 07.46 UT).

The source was serendipitously observed about one year after the SN explosion (in 2016 April) by *Swift*/XRT, which detected the source with an increased count rate of $\simeq 5.0 \times 10^{-2}$ counts s^{-1}. On 2016 September 15th, observing for 7.2 s with the EPIC-pn camera (the *XMM-Newton* observation was in slew mode; see XMMSL1 J073504.6-690752, OBs ID 9307100003), a count rate of 1.7 ± 0.4 counts s^{-1} was observed from the source.

The spectrum was soft,[12] i.e., characterized by an equivalent power-law slope $\Gamma \simeq 3$ or blackbody $kT \simeq 0.13$ keV, and absorbed flux of $F_{0.3-2\,{\rm keV}} = (2.1^{+1.1}_{-1.0}) \times 10^{-12}\,{\rm erg\,cm^{-2}\,s^{-1}}$. The unabsorbed flux, assuming a column density of $2 \times 10^{21}\,{\rm cm^{-2}}$ (Willingale et al. 2013), is $F_{0.3-2\,{\rm keV}} = (7.5^{+3.9}_{-3.5}) \times 10^{-12}\,{\rm erg\,cm^{-2}\,s^{-1}}$, corresponding to a luminosity of

[12] Note, however, that most of the SNe IIn typically have hard X-ray spectra (see, e.g., Chandra et al. 2012a, 2012b; Stritzinger et al. 2012).

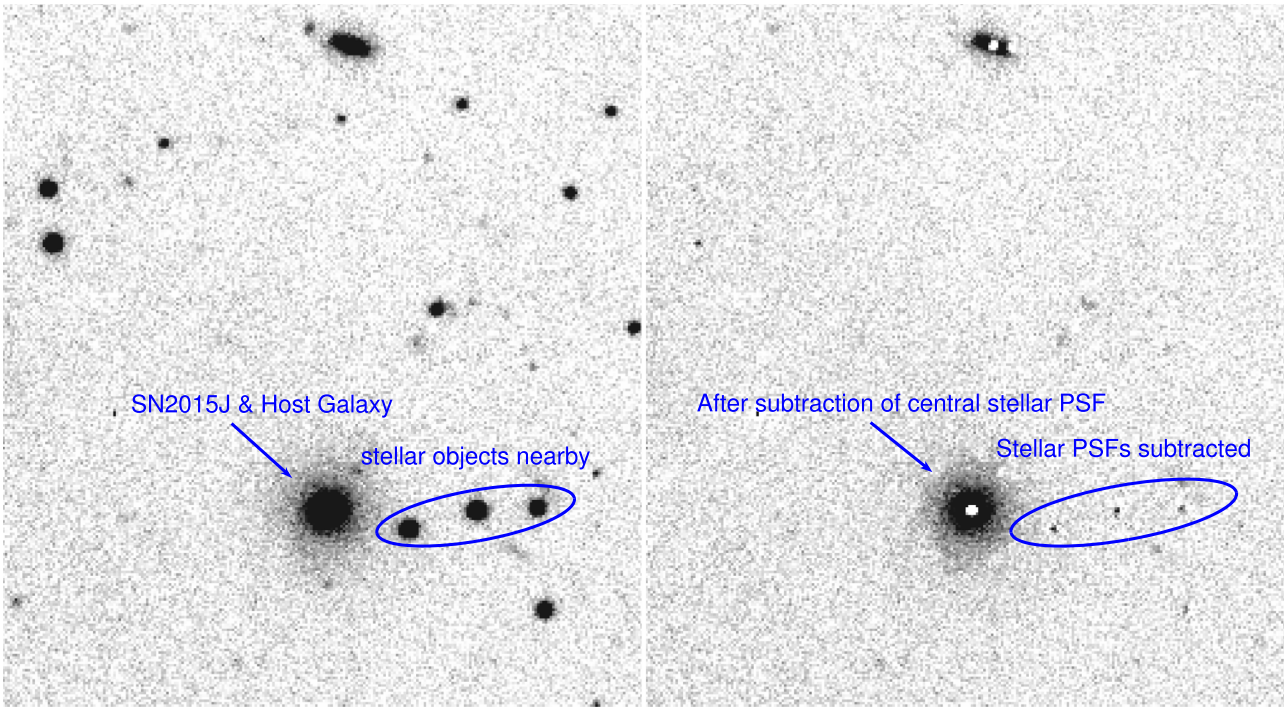

Figure 2. The VLT/FORS2 image of the region around SN 2015J before (left panel) and after (right panel) subtracting the PSF obtained using DAOPHOT. As can be seen, the target source is an extended object, probably a dwarf galaxy (see the text for details).

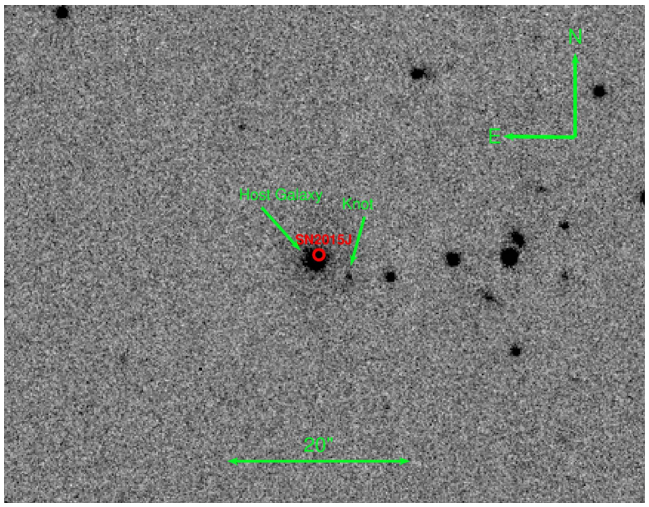

Figure 3. The FourStar *Ks* image of the galaxy host of SN 2015J.

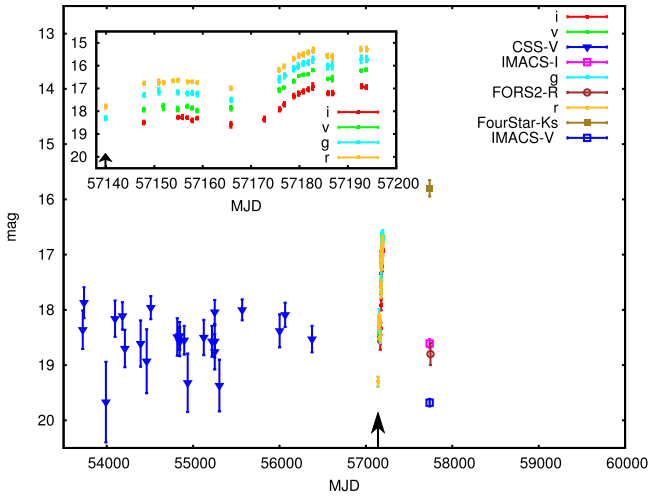

Figure 4. The multi-band light curve of the target, including the CSS data (filled triangles; see the text for details), is shown. The inset shows a zoom-in of the light curve (dots as taken directly from Childress et al. 2015) about the time of the SN event that occurred on 2015 April 27.9 UT (corresponding to MJD = 57139.9, as also indicated by the black arrow). From the *i* band to the *r* band we applied a recursive offset of 0.5 mag for each light curve shown in the inset. The data used to create this figure are available.

$L_{0.3-2\,\mathrm{keV}} = (5.2^{+2.7}_{2.5}) \times 10^{41}\,\mathrm{erg\,s^{-1}}$ for the estimated distance ($\simeq$24.2 Mpc) of the host galaxy.

In order to determine the behavior of the X-ray light curve, we requested new observations of the source by *Swift*/XRT in 2017 March (Obs ID 00033857012) and again in 2017 July (Obs ID 00033857013) and verified that the source is still active in the X-rays at a level of $\simeq 5.4 \times 10^{-2}$ counts $\mathrm{s^{-1}}$. In Figure 5, we show the 0.3–10 keV light curve in terms of the *Swift*/XRT PC count rate, where the *XMM-Newton* slew point has been converted to the *Swift* count rate using the WebPIMMS tool[13] and a power-law spectral model (with $\Gamma = 3$). The X-ray flux has been consistently high between 2016 August and the latest observation in 2017 July.

[13] WebPIMMS is available at https://heasarc.gsfc.nasa.gov/cgi-bin/Tools/w3pimms/w3pimms.pl.

A spectrum was extracted from the 2017 March *Swift* XRT observation and rebinned in order to have at minimum 5 counts per channel with *grppha*. The resulting spectrum (presented in Figure 6) appears to be soft. In fact, assuming an absorbed power law with $nH = 2 \times 10^{21}\,\mathrm{cm^{-2}}$, one gets a power slope of $\Gamma = 4.0 \pm 0.5$ ($\chi^2 = 0.6$ for 15 d.o.f.). The absorbed flux in the 0.3–2 keV band is $(1.1 \pm 0.2) \times 10^{-12}\,\mathrm{erg\,cm^{-2}\,s^{-1}}$, corresponding to an unabsorbed flux of $(6.2 \pm 1.1) \times 10^{-12}\,\mathrm{erg\,cm^{-2}\,s^{-1}}$. The associated luminosity is $L_{0.3-2\,\mathrm{keV}} = (4.3 \pm 0.8) \times 10^{41}\,\mathrm{erg\,s^{-1}}$.

Table 1
Log of the *Swift*/XRT and *XMM-Newton** (11th row) Observations

OBs ID	*T* MJD	Live Time s	Rate count s^{-1}
00033857002	57201.532	1743.12	$(2.7 \pm 1.5) \times 10^{-3}$
00033857003	57204.789	1945.40	$(5.3 \pm 1.8) \times 10^{-3}$
00033857004	57207.045	2349.50	$(4.6 \pm 1.6) \times 10^{-3}$
00033857005	57210.735	1860.50	$(4.6 \pm 1.8) \times 10^{-3}$
00033857006	57221.539	1640.72	$(3.6 \pm 1.6) \times 10^{-3}$
00033857008	57236.589	1937.91	$(3.9 \pm 1.7) \times 10^{-3}$
00033857009	57244.098	1997.83	$(5.9 \pm 1.9) \times 10^{-3}$
00033857010	57252.550	1965.38	$(6.7 \pm 2.0) \times 10^{-3}$
00033857011	57260.324	2017.83	$(7.0 \pm 2.0) \times 10^{-3}$
07002410001	57499.501	59.94	$(5.0 \pm 2.9) \times 10^{-2}$
9307100003*	57646.527	7.2	$(9.0 \pm 3.0) \times 10^{-2}$
00033857012	57820.517	1853.00	$(4.9 \pm 0.5) \times 10^{-2}$
00033857013	57946.721	1313.58	$(5.4 \pm 0.6) \times 10^{-2}$

Note. We give the observation identification number, the (mid) time of exposure, the live time of each observation, and the source count rate in the 0.3–10 keV band.

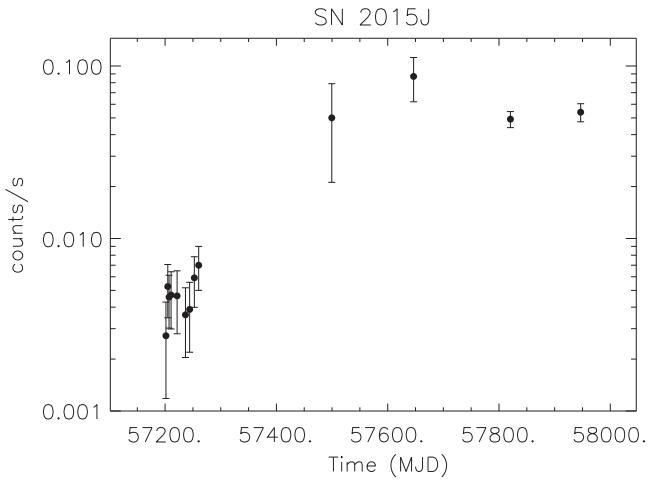

Figure 5. The 0.3–10 keV light curve of SN 2015J. The last data point (acquired by *SWIFT*/XRT in 2017 July) shows that the SN event is still active in the X-rays after more than one year at a level of $\simeq$0.05 counts s^{-1}. The XMM slew flux at MJD = 57646.5 has been converted into a *Swift* count rate (see the text for details).

As far as the last *Swift* XRT observation (2017 July), the spectrum (see Figure 7) can be described by an absorbed power law with $nH = 2 \times 10^{21}\,\mathrm{cm}^{-2}$ and a power slope of $\Gamma = 3.5 \pm 0.5$ ($\chi^2 = 0.7$ for 11 d.o.f.). The absorbed flux in the 0.3–2 keV band is $(1.2 \pm 0.3) \times 10^{-12}\,\mathrm{erg\,cm^{-2}\,s^{-1}}$, corresponding to an unabsorbed flux of $(5.2 \pm 1.3) \times 10^{-12}\,\mathrm{erg\,cm^{-2}\,s^{-1}}$. The associated luminosity is $L_{0.3-2\,\mathrm{keV}} = (3.6 \pm 0.9) \times 10^{41}\,\mathrm{erg\,s^{-1}}$, thus implying an approximately constant X-ray luminosity.

For completeness, the *SWIFT*/UVOT images (in the *U* filter centered at 346.5 nm) were analyzed using the *uvotdetect* and *uvotsource* scripts. By performing aperture photometry with a radius of 5″, we found a *U* magnitude of 19.1 ± 0.1.

4. Results and Discussion

We have presented an analysis of the observations acquired by the VLT (*R* band) and *Magellan* (*V, I*, and *K* bands) telescopes, as well as the X-ray data from the *XMM-Newton* (slew mode) and *Swift* satellites toward the SN 2015J location. Optical and near-IR observations allowed us to discover the SN host galaxy, which appears to be a compact dwarf galaxy with a size of $\simeq$1 kpc at a distance of 24.2 Mpc.

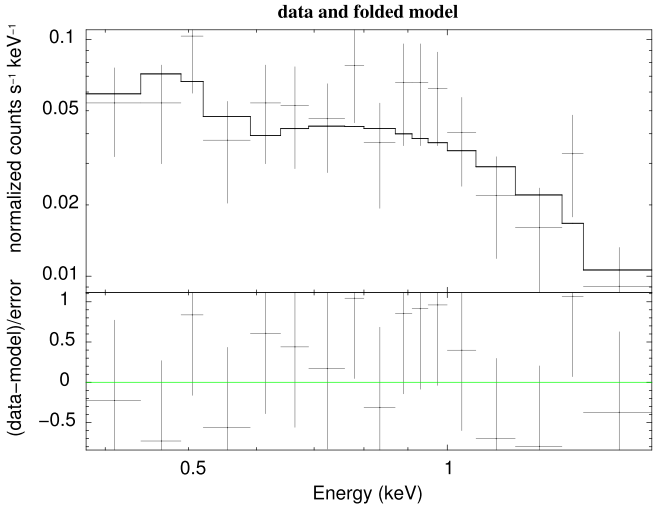

Figure 6. The 0.3–1.7 keV spectrum of SN 2015J as observed by *Swift*/XRT (OBs ID 00033857012).

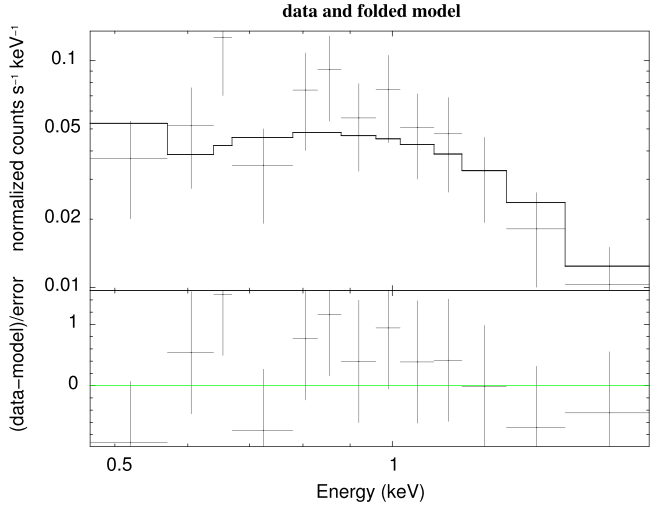

Figure 7. The 0.3–1.7 keV spectrum of SN 2015J as observed by *Swift*/XRT (OBs ID 00033857013).

The X-ray data show that the SN is still active after about two years after the explosion and the derived unabsorbed X-ray luminosity, $L_{0.3-2\mathrm{keV}} \simeq 5.2 \times 10^{41}\,\mathrm{erg\,s^{-1}}$, places SN 2015J among the most luminous young SNe (see Dwarkadas & Gruszko 2012 for a list of SNe observed in X-rays). We note, for comparison, that SN 2010jl was classified as an SN IIn with an unabsorbed 0.2–10 keV luminosity of about $7 \times 10^{41}\,\mathrm{erg\,s^{-1}}$ at 2 and 12 months after the event (Chandra et al. 2012b). Its spectra could be described by a MEKAL model characterized by a high temperature, $kT > 8$ keV, absorbed by a column that dropped from $nH \simeq 10^{24}$ to $nH \simeq 3 \times 10^{23}\,\mathrm{cm}^{-2}$ between the observations. Also, SN-2006jd showed a large X-ray luminosity (about $4 \times 10^{41}\,\mathrm{erg\,s^{-1}}$) for several years after the explosion (Stritzinger et al. 2012). The temperature was also very high here, $kT > 20$ keV, with an intrinsic column of $nH \simeq 10^{21}\,\mathrm{cm}^{-2}$ (Chandra et al. 2012a). In these SNe IIn, the high luminosity has been attributed to a forward shock from ejecta

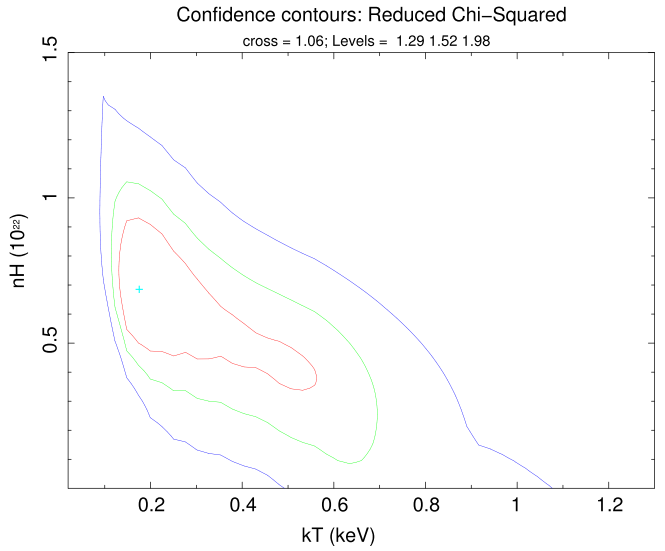

Figure 8. Contour plot of the temperature and absorption column parameters from a fit of an intrinsically absorbed MEKAL model to the *Swift* observation of 2017 July (assuming $z = 0.0054$ and a galactic column density $nH = 2.0 \times 10^{21}\,\mathrm{cm}^{-2}$). The contours mark the 1σ, 2σ and 3σ errors.

expanding at several thousand km s^{-1} into a dense circumstellar medium expelled by the progenitor star in previous shell ejection episodes.

In this respect, we note that SN 2015J has properties in common with these two SNe, particularly the optical spectrum and the X-ray luminosity of a few $\times 10^{41}$ erg s^{-1}, which persisted for more than a year. However, its X-ray spectrum, as deduced from the admittedly low statistics of the *Swift* observations, appears to be much softer than the other SNe IIn. In fact, when fitting the last *SWIFT*/XRT data (2017 July) with an absorbed MEKAL model (i.e., *wabs*zwabs*mekal* within XSPEC, with the *wabs* component accounting for the galactic hydrogen column density and *zwabs* for any intrinsic absorption), the best-temperature is $kT = 0.17^{+0.4}_{-0.04}$ keV (1σ errors), with an upper limit of $\simeq$1.1 keV with a 3σ confidence level (see also Figure 8). Note, however, that the intrinsic column density remains unconstrained (with a maximum allowed value of $\simeq 1.2 \times 10^{22}\,\mathrm{cm}^{-2}$).

A detailed discussion of the evolution of the X-ray light curve from young SNe can be found in Dwarkadas et al. (2010), to whom we refer for more details. Here, we comment that the expansion of an SN shock wave into the ambient medium produces forward and reverse shocks that heat up the gas to sufficiently large temperatures and produce X-rays. The expected X-ray luminosity is then

$$L_X \sim n_e^2 \Lambda V, \tag{1}$$

where n_e is the electron number density, Λ is the cooling function, and V is the volume of gas involved in the emission. Assuming that the surrounding medium number density goes as r^{-s} (with $s = 2$ in the case of a steady wind), that the emission originates from a thin shell with size $\Delta r \propto r$ (as in the self-similar case) at a distance r from the SN, and that $\Lambda \propto r/t$, one gets

$$L_X \sim \frac{r^{4-2s}}{t}. \tag{2}$$

Therefore, the resulting X-ray emission would scale as t^{-1} in the steady wind scenario. Following this discussion, we fitted the last three data points of the 0.3–2 keV light curve assuming a model of the form $L_x = at^b$, where a and b are considered free fit parameters. Fitting the log–log data with the previous relation gave a best fit power-law index $b = -0.98 \pm 1.6$. Although, due to the large associated uncertainty, the light curve is consistent with a flat slope, the central value of the power-law index seems to be reminiscent of a steady wind whose density decreases as r^{-2}.

However, the column density estimated above is far below the value needed to create the X-ray emission. It is possible that we are observing the shocked emission through a hole in the local gas, as suggested in the case of SN 2006jd by Chandra et al. (2012a; see also Katsuda et al. 2016). In addition, the soft spectrum is difficult to reconcile with the high observed X-ray luminosity if it is generated by shocked material, thus presenting other possible interpretations.

For example, one possibility is that some part of the material ejected might have remained bound to the compact remnant and fallen back at later times (see, e.g., Dexter & Kasen 2013).

Alternatively, a tidal disruption event might mimic an SN explosion. For example, the superluminous SN event ASASSN-15lh (Dong et al. 2016) has been reinterpreted as the tidal disruption of a star by a rapidly spinning $10^8\,M_\odot$ black hole by Leloudas et al. (2016) because of the temperature evolution, the total luminosity of the event, and the metal-rich host galaxy. Roughly constant, soft ($\Gamma = 3$ or $kT = 0.17$ keV) X-ray emission has been seen from the position of ASSASN-15lh, with a $L_X \simeq 2$–8×10^{41} erg s^{-1} lasting for several hundred days (Margutti et al. 2017).

The power-law index b of the post-peak SN 2015J X-ray light curve is flatter, but still consistent with the canonical TDE decay curve of $t^{-5/3}$, although we note that more slowly evolving TDE light curves are predicted to be common (Guillochon & Ramirez-Ruiz 2013, 2015).

Therefore, future photometric and high-precision spectroscopic observations in X-rays are important for addressing the issues that still remain open on SN 2015J since, if confirmed, it is one of the brightest SNe II ever observed.

We acknowledge the support by the INFN projects TAsP (Theoretical Astroparticle Physics Project) and EUCLID. We warmly thank the anonymous referee for the suggestions that improved the paper.

ORCID iDs

A. A. Nucita https://orcid.org/0000-0002-7926-3481
F. De Paolis https://orcid.org/0000-0001-6460-7563
R. Saxton https://orcid.org/0000-0002-4912-2477
V. Testa https://orcid.org/0000-0003-1033-1340
F. Strafella https://orcid.org/0000-0002-8757-9371
G. Ingrosso https://orcid.org/0000-0001-6429-5619
K. Boutsia https://orcid.org/0000-0003-4432-5037

References

Arnaud, K., Dorman, B., & Gordon, C. 2007, An X-ray Spectral Fitting Package —User Guide for version 12.4.0, Heasarc Astrophysics Science Division, NASA/GSFC, http://heasarc.gsfc.nasa.gov/docs/xanadu/xspec/
Brown, W. R. 2011, in ASP Conf. Proc. 439, The Galactic Center: A Window to the Nuclear Environment of Disk Galaxies, ed. M. Morris, Q. D. Wang, & F. Yuan (San Francisco, CA: ASP), 246
Brown, W. R., Geller, M. J., & Kenyon, S. J. 2014, ApJ, 787, 89

Brown, W. R., Geller, M. J., Kenyon, S. J., & Kurtz, M. J. 2005, ApJ, 622
Burrows, D. N., Hill, J. E., Nousek, J. A., et al. 2005, SSRv, 120, 165
Chandra, P., Chevalier, R. A., Chugai, N., et al. 2012a, ApJ, 755, 110
Chandra, P., Chevalier, R. A., Chugai, N., Fransson, C., & Soderberg, A. M. 2015, ApJ, 810, 32
Chandra, P., Chevalier, R. A., Irwin, C. M., et al. 2012b, ApJL, 750, L2
Childress, M., Scalzo, R., Yuan, F., et al. 2015, Atel, 7711, 1
Dexter, J., & Kasen, D. 2013, ApJ, 772, 30
Dong, S., Shappee, B. J., Prieto, J. L., et al. 2016, Sci, 351, 257
Dopita, M., Hart, J., McGregor, P., et al. 2007, ApSS, 310, 255
Dwarkadas, V. V., Dewey, D., & Bauer, F. 2010, MNRAS, 407, 812
Dwarkadas, V. V., & Gruszko, J. 2012, MNRAS, 419, 1515
Filippenko, A. V. 1997, ARA&A, 35, 309
Gal-Yam, A., Leonard, D. C., Fox, D. B., et al. 2007, ApJ, 656, 372
Guillochon, J., & Ramirez-Ruiz, E. 2013, ApJ, 767, 25
Guillochon, J., & Ramirez-Ruiz, E. 2015, ApJ, 798, 64
Katsuda, S., Maeda, K., Bamba, A., et al. 2016, ApJ, 832, 194
Leloudas, G., Fraser, M., Stone, N. C., et al. 2016, NatAs, 1, 0002
Margutti, R., Metzger, B. D., Chornock, R., et al. 2017, ApJ, 836, 25
Martin, J. C. 2006, AJ, 131, 3047
Richardson, D., Jenkins, R. L., III, Wright, J., & Maddox, L. 2014, AJ, 147, 118
Ryder, S. D., Kool, E., Stockdale, C. J., & Kotak, R. 2015, Atel, 7762, 1
Ryder, S. D., Koribalski, B., Staveley-Smith, L., et al. 2001, ApJ, 555, 232
Scalzo, R. A., Yuan, F., Childress, M. J., et al. 2017, PASA, 34, 030
Schlegel, E. M. 1990, MNRAS, 244, 269
Stetson, P. B. 1987, PASP, 99, 191
Stritzinger, M., Taddia, F., Fransson, C., et al. 2012, ApJ, 756, 173
Tsvetkov, D. Y., Pavlyuk, N. N., & Bartunov, O. S. 2004, AstL, 30, 729
Willingale, R., Starling, R. L. C., Beardmore, A. P., Tanvir, N. R., & O'Brien, P. T. 2013, MNRAS, 431, 394
Wright, E. L., Eisenhardt, P. R. M., Mainzer, A. K., et al. 2010, ApJ, 140, 1868
Zinn, P.-C., Stritzinger, M., Braithwaite, J., et al. 2012, A&A, 538, 30